

## Article

# Effects of Oxygen Partial Pressure and Thermal Annealing on the Electrical Properties and High-Temperature Stability of Pt Thin-Film Resistors

Yawen Pang<sup>1,†</sup>, Nan Zhao<sup>1,†</sup> , Yong Ruan<sup>2</sup>, Limin Sun<sup>3</sup> and Congchun Zhang<sup>1,\*</sup>

<sup>1</sup> National Key Laboratory of Science and Technology on Micro/Nano Fabrication, Shanghai Jiao Tong University, Shanghai 200240, China

<sup>2</sup> State Key Laboratory of Precision Measurement Technology and Instruments, Department of Precision Instrument, Tsinghua University, Haidian District, Beijing 100084, China

<sup>3</sup> Instrumental Analysis Center of Shanghai Jiao Tong University, Shanghai 200240, China

\* Correspondence: zhcc@sjtu.edu.cn

† These authors contributed equally to this work.

**Abstract:** The effects of oxygen partial pressure and annealing temperature on the microstructure, electrical properties, and film adhesion of Pt thin-film resistors with Pt<sub>x</sub>O<sub>y</sub> as the adhesion layer were investigated. Pt/Pt<sub>x</sub>O<sub>y</sub> films were deposited on alumina substrates by radio frequency sputtering and annealed in a muffle furnace at temperatures in the range of 800–1000 °C. The microstructure and chemical composition of Pt thin-film resistors were examined by optical microscopy, scanning electron microscopy, X-ray photoelectron spectroscopy, and time-of-flight secondary ion mass spectrometry. The experimental results show that annealing will lead to the formation of bubbles on the surface of the film, and the film prepared at 20% oxygen partial pressure has the least bubbles. The Pt thin-film resistors with a Pt<sub>x</sub>O<sub>y</sub> adhesion layer sputtered with 10% oxygen partial pressure had the highest TCR (temperature coefficient of resistance) of 3434 ppm/°C, and the TCR increased with increasing annealing temperature. Repeated experiments show that Pt thin-film resistors have better stability at annealing temperatures of 800 °C and 900 °C. Comprehensively considering the TCR and stability, the optimal adhesion layer of Pt thin-film resistors was prepared at an oxygen partial pressure of 10% and an annealing temperature of 900 °C.

**Keywords:** Pt thin-film resistor; platinum oxide adhesion layer; microstructure; TCR; high-temperature stability



**Citation:** Pang, Y.; Zhao, N.; Ruan, Y.; Sun, L.; Zhang, C. Effects of Oxygen Partial Pressure and Thermal Annealing on the Electrical Properties and High-Temperature Stability of Pt Thin-Film Resistors.

*Chemosensors* **2023**, *11*, 285.

<https://doi.org/10.3390/chemosensors11050285>

chemosensors11050285

Academic Editor: Marco Frasconi

Received: 4 March 2023

Revised: 26 April 2023

Accepted: 8 May 2023

Published: 10 May 2023



**Copyright:** © 2023 by the authors. Licensee MDPI, Basel, Switzerland. This article is an open access article distributed under the terms and conditions of the Creative Commons Attribution (CC BY) license (<https://creativecommons.org/licenses/by/4.0/>).

## 1. Introduction

Thin-film resistance temperature detectors (RTDs) have been widely used in the industry due to the advantages of small size, simple structure, and fast response [1–3]. A variety of heat-sensitive materials are available for different applications, and platinum (Pt) is the best choice for high-precision measurement over a wide range of temperatures because of its high temperature coefficient of resistance (TCR) and reliable performance [2,4–7]. However, the mismatching between the Pt film and the substrate (such as Al<sub>2</sub>O<sub>3</sub>, SiO<sub>x</sub>, or SiN<sub>x</sub>) results in very poor adhesion. The adhesion of the deposited film to the oxide substrate is related to the free energy of the oxide during deposition, and it is generally believed that the higher the free energy, the stronger the adhesion [8]. Therefore, to improve adhesion, an adhesion layer such as titanium (Ti), tantalum (Ta), or chromium (Cr) is a common solution, and they can reduce the mismatch between the Pt film and substrate properties and enhance film adhesion. While at high temperature (>650 °C), these metallic adhesion layers tend to oxidation, interdiffusion or reaction with the substrate leads to the increase in resistance and the reduction in the TCR and stability [2,9–16].

In order to solve the problem of high-temperature oxidation of metallic adhesion layers, many researchers used metal oxide as adhesion layers. Garraud et al. studied

the thermal stability of the adhesion layers of Pt/Cr and Pt/Cr<sub>2</sub>O<sub>3</sub> films based on the SiN/Si temperature sensors and found that the Pt/Cr<sub>2</sub>O<sub>3</sub> film has smaller resistance drift, which indicates that the adhesion layer will affect the relative temperature measurement performance and resistance drift rate of Pt thermal resistance, which can be explained by the oxygen in the adhesion layer that prevented the diffusion of Cr [17]. Jae-suk lee reported that the (Al, Si) oxide layer as an adhesion promoting layer provided excellent adhesion between Pt and the substrate [7], but it was found that the Pt film occurred agglomeration at high temperatures. Chung et al. prepared Pt resistors using MgO as an adhesion layer with a TCR of 3927 ppm/°C and a ratio of resistance values that linearly varied over the temperature range of 25–400 °C [18]. Some studies have been carried out by depositing Pt<sub>x</sub>O<sub>y</sub> as an adhesion layer to enhance film adhesion. Pt<sub>x</sub>O<sub>y</sub> can be prepared by reactive magnetron sputtering under O<sub>2</sub>/Ar gas mixtures [19]. Budhani researched the effects of the Pt<sub>x</sub>O<sub>y</sub> adhesion layer of Pt films on alumina substrates and found that Pt/Pt<sub>x</sub>O<sub>y</sub>/Al<sub>2</sub>O<sub>3</sub> showed stronger adhesion than pure Pt films even after several thermal cycles at 1000 °C [20]. Tsutsumi K. prepared Pt thin-film resistors with a SiNx and Al<sub>2</sub>O<sub>3</sub> adhesion layer on silicon oxide wafer and studied the effect of annealing on its performance. It was found that after annealing at 1100 °C, the TCR of the sample was as high as  $3.7 \times 10^{-3}/^{\circ}\text{C}$  [4]. NASA prepared a Pt thin-film resistor with Pt<sub>x</sub>O<sub>y</sub> as the adhesion layer. The influences of sputtering power, pressure, and annealing conditions on film stress, heat loss, resistivity, and film adhesion were studied, but the effect of oxygen partial pressure and annealing temperature on Pt thin-film resistors and stability with Pt<sub>x</sub>O<sub>y</sub> as the adhesion layer was not reported [21]. M. Grosser prepared Pt film thermal resistance with a titanium adhesion layer on silicon oxide wafer and found that annealing can improve the resistivity and other related electrical properties of thermal resistance [22]. Timo Schossler fabricated a multilayer temperature sensor with a Pt film as the functional layer on a silicon oxide substrate by magnetron sputtering. They found that the resistivity of the sample decreased from  $16.8 \pm 0.4 \mu\Omega$  to  $12.7 \pm 0.2 \mu\Omega$  after annealing at 800 °C. The TCR increased from 2180 ppm/K to 2810 ppm/K. The temperature measurement performance of thermal resistance is improved [23].

In this work, Pt/Pt<sub>x</sub>O<sub>y</sub> resistance films were deposited by magnetron sputtering, including Pt films deposited in pure argon and Pt<sub>x</sub>O<sub>y</sub> adhesion layer films deposited by reactive sputtering in O<sub>2</sub>/Ar gas mixtures, while oxygen partial pressures were 5%, 10%, 15%, 20%, and 50%. Then, the resistors were annealed at 800 °C, 900 °C, and 1000 °C, respectively. After that, we studied the microstructure, electrical properties, high-temperature stability, and film adhesion of Pt thin-film resistors. Then the microstructure and chemical composition were characterized, and we discussed the effects of the mechanisms of the TCR and stability. Furthermore, the film adhesion characterized by a nanometer scratch meter was tested. This work may provide reference for subsequent work on RTDs.

## 2. Materials and Methods

### 2.1. Pt Thin-Film Resistor Preparation

First of all, a 3-inch-diameter single-polished alumina ceramic substrate was cleaned with nanometer calcium carbonate to ensure uniform grinding in all areas, followed by rinsing with deionized water, so that the water can be completely wetted; there were no aggregated water droplets on the surface; the process was correspondingly followed by ultrasonic cleaning with deionized water, 5% sodium hydroxide, and potassium dichromate solution. Then the Pt thin-film resistor was fabricated by microlithography and lift-off process. The process schematic was given in Figure 1a–e. A positive photoresist of AZ-4620 was spin-coated onto the alumina substrate and baked at 90 °C for 2 h. The resistor pattern was transferred after exposure for 40 s under the i-line from a mercury arc lamp with a constant intensity of  $8 \text{ mW}\cdot\text{cm}^{-2}$ . The substrate was then immersed in a developer solution. Afterward, the substrate was rinsed with deionized water to remove the remaining developer and then baked at 90 °C for 30 min.

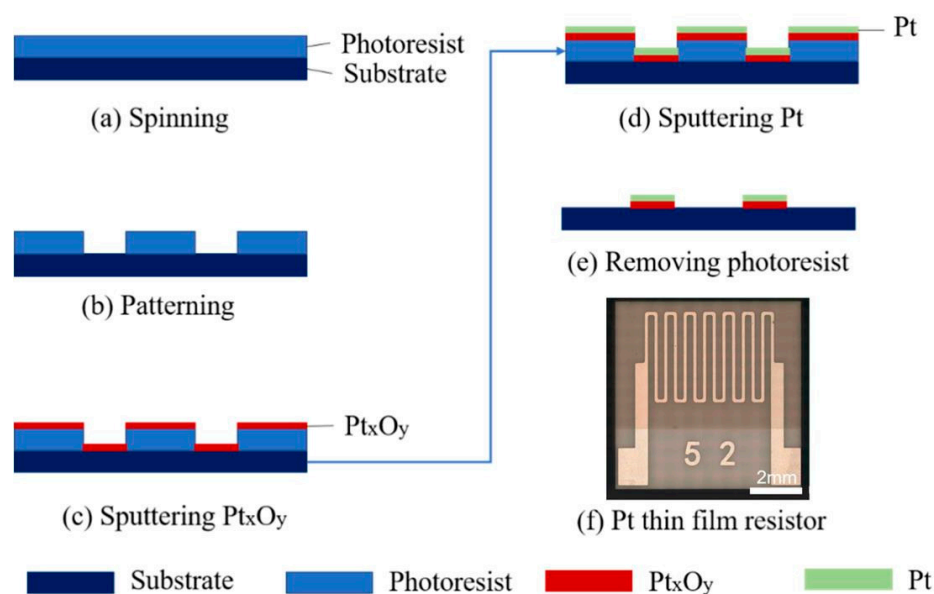


**Figure 1.** Fabrication process (a–e) and overall morphology (f) of Pt thin-film resistor.

The  $Pt_xO_y$  adhesion layer was deposited by reactive magnetron sputtering (MSP-400, China) using a Pt target (99.99%) with a diameter of 100 mm in  $O_2/Ar$  gas mixtures with an oxygen partial pressure ranging from 5% to 50%. Then, a Pt film was deposited by radio frequency (RF) sputtering in pure Ar atmosphere. The base and sputtering pressures were  $5 \times 10^{-4}$  Pa and 0.5 Pa, respectively. The  $Pt_xO_y$  adhesion layer and Pt film have the same sputtering power of 150 W and different depositing times of 5 min and 8 min, respectively. The deposition rates of various oxygen partial pressures are listed in Table 1. Pt/ $Pt_xO_y$  films were structured by a lift-off process. After being rinsed with deionized water and dried with  $N_2$ , the substrate was cut into several small pieces ( $7.5 \text{ mm} \times 7.1 \text{ mm} \times 0.6 \text{ mm}$ ) by laser cutting equipment, as illustrated in Figure 1f. The Pt RTDs were annealed in a muffle furnace at different temperatures (800–1000 °C) for 2 h with a heating rate of 5 °C/min and then naturally cooled.

**Table 1.** Deposition rate of  $Pt_xO_y$  and Pt film adhesion layer prepared with various oxygen partial pressures.

Film	$Pt_xO_y$ Adhesion Layer					Pt Film
	5%	10%	15%	20%	50%	
Oxygen partial pressure	5%	10%	15%	20%	50%	-
Deposition rate (nm/min)	$33 \pm 4$	$34 \pm 3$	$36 \pm 3$	$55 \pm 3$	$60 \pm 4$	$48 \pm 3$

## 2.2. Characterization of Resistor

(1) Digital microscopy (Keyence, VHX-5000, Japan), scanning electron microscopy (SEM, Zeiss Ultra55, Germany), and focused ion beam (FIB, Zeiss Auriga SEM/FIB cross-beam System, Germany) were used to characterize the surface and cross-sectional microstructure. Polyfunctional X-ray diffraction (XRD, Bruker 3 kW/D8 ADVANCE Da Vinci, Germany) was applied to measure crystallinity and full width at half-maximum (FWHM) with  $Cu K\alpha$  radiation ( $\lambda = 1.5406 \text{ \AA}$ ) operated at 40 kV and 40 mA. X-ray photoelectron spectroscopy (XPS) with a monochromatic  $Al K\alpha$  source (1486.6 eV) was used to characterize the surface chemical composition of the Pt film. Pass energies of 160 eV and 40 eV were used for survey spectra and narrow scan spectra with energy step sizes of 1 eV and 0.1 eV, respectively. The binding energy scale was calibrated according to the C 1s peak (284.8 eV) of adventitious carbon on the analyzed sample surface. Time-of-flight secondary ion mass spectrometry (TOF-SIMS, ION TOF TOF-SIMS 5-100, Germany) was used to characterize the three-dimensional and spatial scale chemical composition distribution.

(2) For a standard Pt100 resistor, the dependence of resistance on temperature was described as follows:

$$R_T = R_0(1 + AT + BT^2) \quad 0^\circ\text{C} < T < 850^\circ\text{C} \quad (1)$$

where A and B were fitting constants, and  $R_0$  was the resistance at  $0^\circ\text{C}$ . At low temperature ( $0\text{--}200^\circ\text{C}$ ), B was negligible because the resistance temperature curve (R–T curve) had high linearity with a coefficient of determination of linear regression greater than 0.9999.

The average TCR was calculated as follows:

$$\text{TCR} = \alpha = (R_{T_2} - R_{T_1}) / (R_{T_1} \cdot (T_2 - T_1)) = \Delta R / \Delta T \cdot R_{T_1} \quad (2)$$

where  $\Delta R / \Delta T$  was the slope of the R–T curve, and  $R_{T_1}$  corresponded to the resistance at  $20^\circ\text{C}$ . It should be noted that this R–T curve referred to the first temperature test for the annealed resistor. To obtain the temperature dependence of the resistance, each resistor was measured by a  $6_{1/2}$  digital Agilent multimeter (Agilent, Keysight 34464A, USA), and the resistor temperature was controlled by an intelligent thermostatic oil bath with methyl silicone as the medium between  $20$  and  $150^\circ\text{C}$ . The heating rate of the intelligent thermostatic oil bath was approximately  $2^\circ\text{C}/\text{min}$ . The temperature was raised in increments of  $10^\circ\text{C}$  and held for 5 min after each increase. During the holding time, the data were recorded.

The stability of the resistor was characterized by the change rate of  $R_{T_1}$  after 4 tests of R–T curves. The R–T curve was obtained through a data acquisition system (Agilent, Keysight DAQ970A, USA) and muffle furnace at test temperatures from room temperature to  $800^\circ\text{C}$  with a heating rate of  $5^\circ\text{C}/\text{min}$ . In the testing process, the muffle is used to provide a high-temperature environment, the R-type thermocouple is used to calibrate the furnace temperature, and the Pt RTDs' resistance is output through DAQ970A.

### 3. Results and Discussion

We prepared the  $\text{Pt}_x\text{O}_y$  adhesion layer made with oxygen partial pressures of 5%, 10%, 15%, 20%, and 50% and then annealed in a muffle furnace up to  $800^\circ\text{C}$ ,  $900^\circ\text{C}$ , and  $1000^\circ\text{C}$  for 2 h to investigate the influential mechanisms of oxygen partial pressure and annealing temperature.

#### 3.1. Microstructure and Chemical Composition

The morphologies of the as-deposited and annealed Pt/ $\text{Pt}_x\text{O}_y$ / $\text{Al}_2\text{O}_3$  resistors with different oxygen partial pressure and annealed temperature in the adhesion layer are shown in Figure 2 [24].

Figure 2a shows that the defects on the surface of the as-deposited film were caused by rough substrates. Compared with the as-deposited films, blisters with diameters in the range of  $2\ \mu\text{m}$  to  $20\ \mu\text{m}$  were observed, and they were irregularly distributed on the surface of the annealed films. As the oxygen partial pressure increased from 5% (Figure 2b) to 10% (Figure 2c), the number of bumps sharply increased. When the oxygen partial pressure increased from 15% to 50% (Figure 2d–f), the blisters that formed on the surface of the Pt film significantly decreased. At an oxygen partial pressure of 15% (Figure 2d), the number of bumps drastically decreased compared with that at 10%. When the oxygen partial pressure increased to 20% (Figure 2e), the bumps were almost unnoticeable. As the oxygen partial pressure increased to 50% (Figure 2f), there were some bumps on the surface of the Pt/ $\text{Pt}_x\text{O}_y$  film. Kwon et al. and Hummel et al. also observed blisters in the Pt film, and they assumed that the formation of bubbles is due to the Ar collection at the film–substrate interface. However, the diffusion of Ar atoms over the micron-scale distances required to collect Ar at a blister location seems unlikely. Compared with Figure 2a, there is no blister formation.

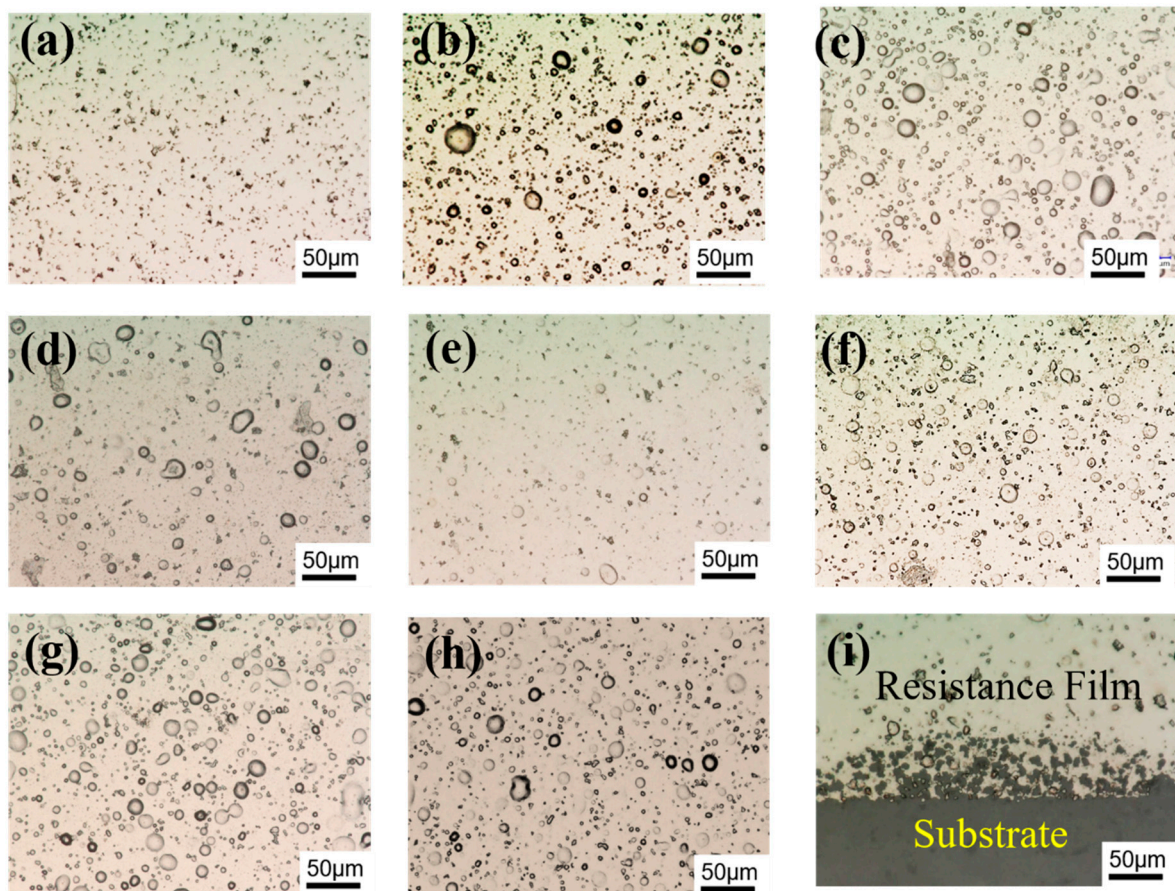


**Figure 2.** (a) Morphologies of the as-deposited resistance film and resistance films with adhesion layer prepared with oxygen partial pressure of (b) 5%, (c) 10%, (d) 15%, (e) 20%, and (f) 50% annealed at 800 °C. Resistance films prepared with 10% oxygen partial pressure in the adhesion layer annealed at (g) 900 °C and (h) 1000 °C. (i) Edge of (h) [24].

For a given oxygen partial, as the annealing temperature increased from 800 °C to 1000 °C (Figure 2c,g,h), the number of blisters first increased and then decreased. The above phenomenon can be explained that with the increase in the annealing temperature, the decomposition of  $Pt_xO_y$  intensifies, more  $O_2$  escapes, and the number of bubbles on the surface of the thin film increases. As the annealing temperature continued to increase, the  $Pt_xO_y$  content decreased and the decomposition weakened. As the grain size increased, the defects were eliminated, and the bubbles were repaired due to the grain growth; then the number of bubbles decreased.

Figure 2i showed the edge of the Pt/ $Pt_xO_y$  film annealed at 1000 °C. Film agglomeration and voids were observed, which agreed with the phenomena reported in previous research. It was reported that the capillary action produced by the high specific surface area of the film was the main reason for the agglomeration. Films always have defects or pinholes [25]. When the radius of the defect was larger than the thermodynamic critical radius determined by the film thickness and wetting angle, the defect grew through capillary action until it was stable [26,27]. Longer exposure time and higher temperature would increase agglomeration, which increased the resistance and was harmful for devices [25,28].

The cross-section morphologies of a blister are shown in Figure 3a. The wall thickness was not uniform, and a gap ( $\sim 2 \mu m$ ) was formed between the film and substrate, which may be due to gas escape during annealing. The  $Pt_xO_y$  adhesion layer prepared by reactive RF sputtering was composed of Pt, PtO, and PtO<sub>2</sub>. Earlier studies indicated that PtO<sub>2</sub> began to break down at 550 °C to form O<sub>2</sub>, PtO, and Pt. PtO<sub>2</sub> and PtO continued to decompose into Pt and O<sub>2</sub> with increasing temperature [28], and all Pt–O compounds

completely dissociated into Pt at 1100 °C [29,30]. Therefore, the blisters may be caused by the decomposition of the  $Pt_xO_y$  adhesion layer and oxygen escape. The focused ion beam (FIB) results of the surface are shown in Figure 3b.

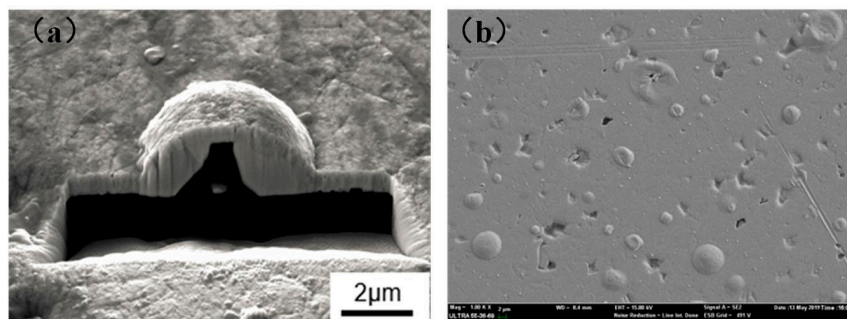


**Figure 3.** (a) Cross-section of a blister; (b) FIB of surface.

Figure 4 showed the wide scan and Pt XPS spectra of the as-deposited Pt/ $Pt_xO_y$  film. The binding energies of the Pt 4f<sub>7/2</sub> and Pt 4f<sub>5/2</sub> peaks were 70.9 eV and 74.2 eV, respectively, which agreed with the reported values of 70.3 eV and 73.68 eV for a pure Pt film [19]. It is verified that the upper layer of the Pt/ $Pt_xO_y$ /Al<sub>2</sub>O<sub>3</sub> resistor was Pt.

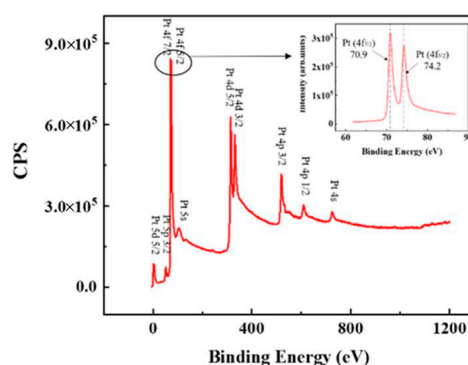


**Figure 4.** Wide scan and Pt XPS spectra of the as-deposited Pt/ $Pt_xO_y$  film.

To test our assumption of blisters resulting from the decomposition of  $Pt_xO_y$ , TOF-SIMS depth profiling experiments were conducted on the as-deposited and annealed Pt/ $Pt_xO_y$ /Al<sub>2</sub>O<sub>3</sub> resistors with the adhesion layer prepared with 10% oxygen partial pressure. The depth profiling plots and 3D rendered images of ions Pt<sup>-</sup>, PtO<sup>-</sup>, PtO<sub>2</sub><sup>-</sup>, and AlO<sup>-</sup> for the as-deposited and annealed films were constructed from raw data and are given in Figure 5.

Figure 5a showed the peak intensity changes of ions (Pt<sup>-</sup>, PtO<sup>-</sup>, PtO<sub>2</sub><sup>-</sup>, and AlO<sup>-</sup>) with the sputtering time that corresponded to the depth, and the longer the sputtering time was, the deeper the depth was. Pt<sup>-</sup> ions represented the existence of Pt-containing materials, such as metallic Pt and platinum oxide, while PtO<sup>-</sup> and PtO<sub>2</sub><sup>-</sup> ions indicated the presence of a platinum oxide layer, and the AlO<sup>-</sup> ion represented the Al<sub>2</sub>O<sub>3</sub> substrate. From Figure 5a, the interface of the resistance film and Al<sub>2</sub>O<sub>3</sub> substrate was clear at a sputtering time of approximately 1860 s, and the  $Pt_xO_y$  adhesion layer was located at a depth reached between approximately 1500 s and 1860 s; then sputtering time from 0 s to approximately 1500 s corresponded to Pt. This suggested that there is a  $Pt_xO_y$  adhesion layer between the Pt film and Al<sub>2</sub>O<sub>3</sub> substrate, forming a sandwich structure of Pt/ $Pt_xO_y$ /Al<sub>2</sub>O<sub>3</sub>, which was more directly revealed by the 3D rendering images in Figure 5b.

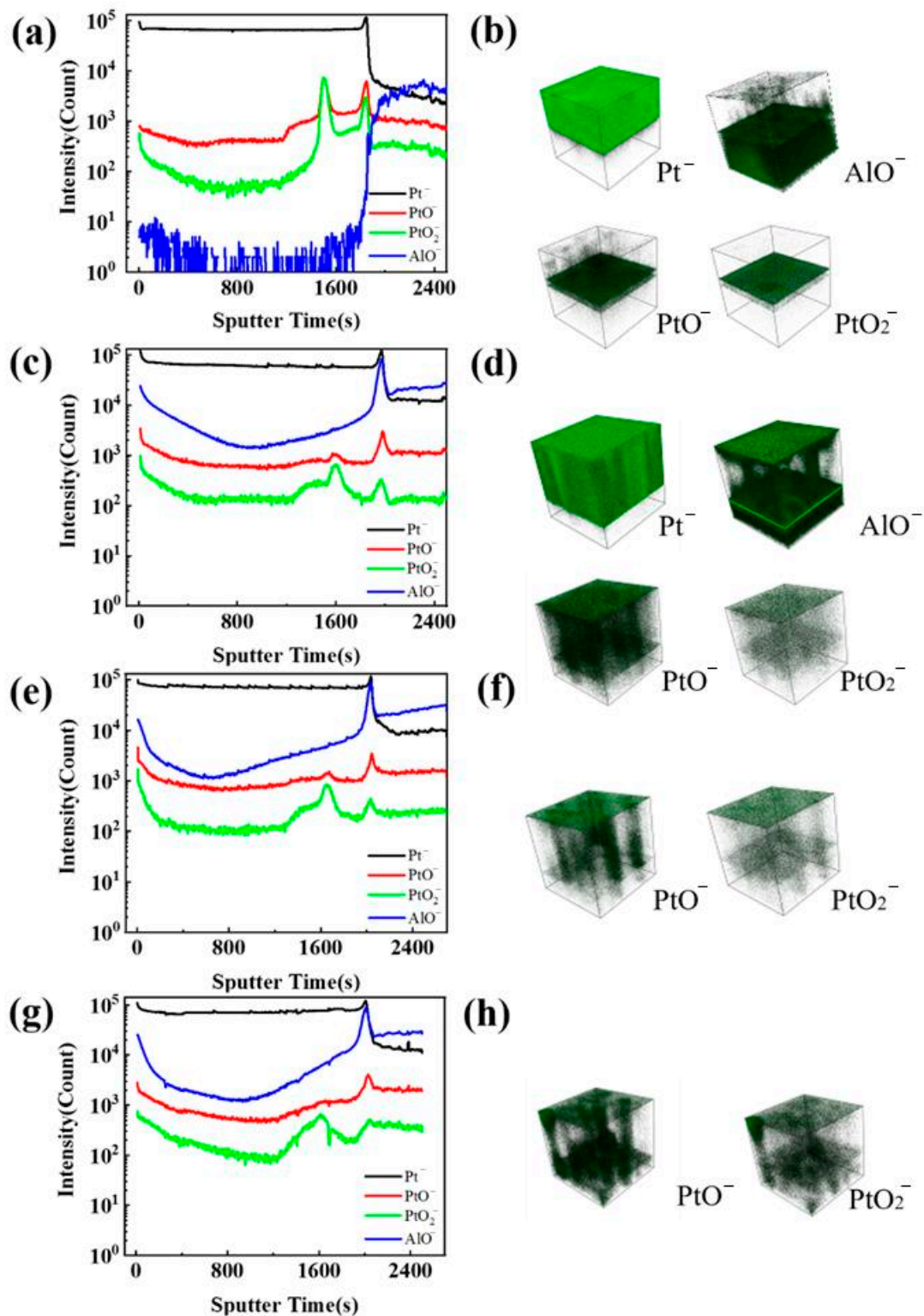


**Figure 5.** Depth profiling plots (a,c,e,g) and 3D rendered images (b,d,f,h) of ions  $Pt^-$ ,  $PtO^-$ ,  $PtO_2^-$ , and  $AlO^-$  for the as-deposited resistance films (a,b) and resistance films annealed at 800 °C (c,d), 900 °C (e,f), and 1000 °C (g,h).

For the annealed films, as shown in Figure 5c,e,g, the  $PtO_2^-$  and  $PtO^-$  ion peak intensities and their distribution widths were much lower and wider than those of the as-deposited film (Figure 5a), indicating that the annealing thins the  $Pt_xO_y$  adhesion layer and intensifies the diffusion. This phenomenon could also be easily found from Figure 5b,d,h.

Additionally,  $\text{AlO}^-$  ions appeared to penetrate the upper Pt layer after annealing, as Figure 5d shows, which suggested that  $\text{Al}_2\text{O}_3$  will diffuse to Pt. With increasing annealing temperature, the intensity of  $\text{PtO}_2^-$  and  $\text{PtO}^-$  first decreased and then slightly increased, and the interface of the  $\text{Pt}_x\text{O}_y$  adhesion layer gradually blurred.

X-ray diffraction pattern of the as-deposited and annealed resistance films was obtained, as illustrated in Figure 6. Compared with the as-deposited film, the spectra showed an obvious increase in the intensity of the Pt (111) peak in the 800 °C annealed resistance film, which revealed an increase in crystallinity. With increasing annealing temperature, Pt oxidation got serious and the lattice constant decreased, which caused the Pt (111) peak to shift to a larger  $2\theta$ .

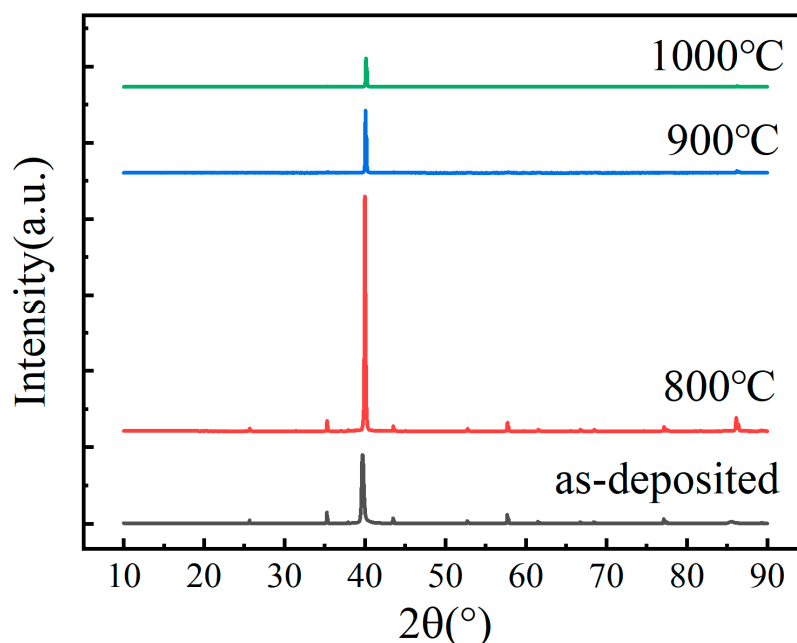


**Figure 6.** X-ray diffractograms of the as-deposited and annealed resistance films.

In addition, oxidation, film heat loss, agglomeration, and diffusion contributed to the drastic reduction in the intensity of the Pt (111) peak. The FWHMs of the Pt (111) peak in the as-deposited resistance film and resistance films annealed at 800 °C, 900 °C, and 1000 °C were evaluated as 0.290°, 0.136°, 0.094°, and 0.116°, which indicated that grain growth occurred as the annealing temperature increased.

### 3.2. Electrical Properties and High-Temperature Stability

To investigate the effect of oxygen partial pressure and annealing temperature on the Pt RTDs' electrical properties, the resistance change rate was investigated, as shown in Table 2. It should be noted that due to experimental error, the resistance of resistors fabricated by the same process on the same substrate is not the same, and the standard deviation is about 10 Ω. In this work, resistors with similar resistances ( $\pm 5 \Omega$ ) were selected for testing, and the test results were the average of 5 specimens.

**Table 2.** Effects of oxygen partial pressure and annealing temperature on Pt/Pt<sub>x</sub>O<sub>y</sub>/Al<sub>2</sub>O<sub>3</sub> resistors.

Oxygen Partial Pressure	5%	10%	15%	20%	50%	
Resistance at RT (as-deposited) ( $\Omega$ )	130.6 $\pm$ 3.5	146.9 $\pm$ 4.3	177.5 $\pm$ 4.3	196.3 $\pm$ 4.8	155.4 $\pm$ 4.6	
Annealing temperature and resistance change rate	800 °C	−19.8%	−32.4%	−41.0%	−45.9%	−47.9%
	900 °C	−19.0%	−32.9%	−34.3%	−44.9%	−49.0%
	1000 °C	−17.6%	−32.6%	−34.1%	−43.7%	−49.1%

Note: All resistance change rate had standard deviation less than 0.03.

With increasing oxygen partial pressure, the initial resistance of the as-deposited resistors first increased and then decreased. The resistance decreased after annealing, and the larger the oxygen partial pressure was, the more the resistance decreased. For Pt/Pt<sub>x</sub>O<sub>y</sub>/Al<sub>2</sub>O<sub>3</sub> resistors prepared with fixed oxygen partial pressure, the annealing temperature has little effect on the rate of resistance change. Resistors with an adhesion layer prepared with 10% oxygen partial pressure showed the most stable change rate in the entire annealing temperature range.

The TCR is a key parameter for characterizing Pt resistance. There are many parameters that influence the TCR, such as crystal characteristics, void formation, the nature of the substrate, interdiffusion of adhesion layers, etc. [31,32]. Figure 7 depicts the TCR versus oxygen partial pressure and annealing temperature. Error bars represented the standard deviation. The TCR increased with increasing annealing temperature but did not monotonically vary with an increase in the oxygen partial pressure. The variation trend of resistors annealed at different temperatures was similar. For example, at 800 °C, the TCR increased from 3371 ppm/°C to 3390 ppm/°C as the oxygen partial pressure increased from 5% to 10%. When the oxygen partial pressure increased further, however, the TCR began to decrease. For resistors with an adhesion layer prepared with 15% oxygen partial pressure, the TCR was 3327 ppm/°C, and when the oxygen partial pressure was raised to 20%, it dropped to 3285 ppm/°C due to large resistance. As it increased to 50%, the TCR returned to 3320 ppm/°C. The largest TCR was 3434 ppm/°C, which corresponded to the Pt thin-film resistors with an adhesion layer prepared with 10% oxygen partial pressure and annealed at 1000 °C. It can be explained that with increasing oxygen partial pressure, the Pt<sub>x</sub>O<sub>y</sub> content in the adhesion layer increased, which directly led to an increase in resistance. Although Pt<sub>x</sub>O<sub>y</sub> decomposed during annealing, there was still a considerable amount of Pt<sub>x</sub>O<sub>y</sub> when oxygen partial pressure was above 10%, and the resistance was large, leading to a small TCR. On the other hand, a high oxygen concentration in sputtering was harmful due to more anomalies and discoloration [21], which resulted in an increase in resistivity and a decrease in the TCR because the product of resistivity and the TCR was constant [33]. The unexpected phenomenon of the resistor with an adhesion layer prepared with 50% oxygen partial pressure was not clear and may be related to the oxidation of Pt in the target surface becoming saturated.

Stability is an important performance parameter for thin-film resistors. The R–T curves of resistors with an adhesion layer prepared with 10% oxygen partial pressure and annealed at 800 °C, 900 °C, and 1000 °C were tested. Resistance operating temperature should not be higher than annealing temperature. Based on this, each test was carried out for 4 cycles up to 800 °C, and the curves are shown in Figure 8.

The resistance of all resistors slightly increased with the change rates of 0.14%, 0.13%, and 0.4%, corresponding to resistors annealed at 800 °C, 900 °C, and 1000 °C, respectively. It was clear that the R–T curves of resistors annealed at 800 °C and 900 °C had better repeatability than those of resistors annealed at 1000 °C, which showed an obvious shift as the experiment proceeded. Then we can conduct that the resistor prepared with an oxygen partial pressure of 10% and annealed at 900 °C owned a high TCR and good stability.

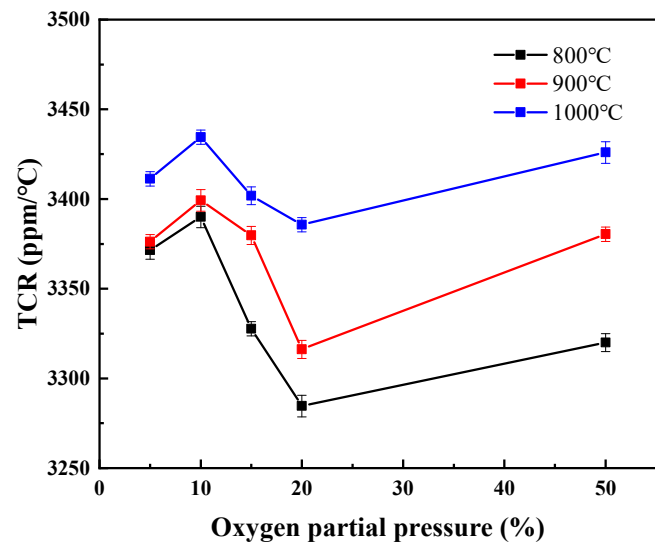


Figure 7. TCR curves of Pt/Pt<sub>x</sub>O<sub>y</sub>/Al<sub>2</sub>O<sub>3</sub> resistors annealed at 800 °C, 900 °C, and 1000 °C for 2 h.

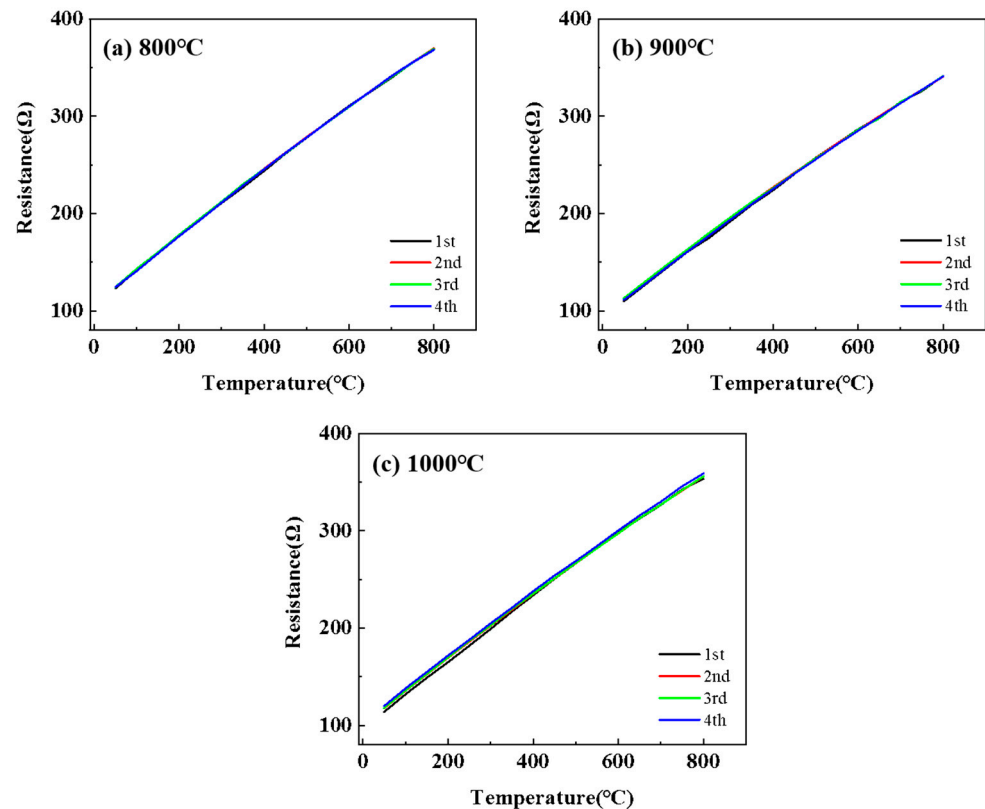


Figure 8. R–T curves of Pt/Pt<sub>x</sub>O<sub>y</sub>/Al<sub>2</sub>O<sub>3</sub> resistors with adhesion layer prepared with 10% oxygen partial pressure annealed at 800 °C (a), 900 °C (b), and 1000 °C (c).

#### 4. Conclusions

For Pt thin-film resistors with a Pt<sub>x</sub>O<sub>y</sub> adhesion layer, the influence of the annealing temperature (800 °C, 900 °C, and 1000 °C) and oxygen partial pressure (5%, 10%, 15%, 20%, and 50%) on the film microstructure, electrical properties, stability, and film adhesion was investigated. Then the Pt thin-film resistor was fabricated by microlithography and lift-off process and prepared by reactive magnetron sputtering. After annealing, Pt<sub>x</sub>O<sub>y</sub> decomposed and bubbles formed on the surface of the Pt thin film. In addition, the resistance decreased after annealing, and the higher the oxygen partial pressure was, the

greater the resistance decreased. The Pt thin-film resistor with a Pt<sub>x</sub>O<sub>y</sub> adhesion layer sputtered at 10% oxygen partial pressure and annealed at 1000 °C had the largest TCR (3434 ppm/°C). The resistors annealed at 800 °C and 900 °C had better stability than those annealed at 1000 °C. The Pt<sub>x</sub>O<sub>y</sub> adhesion layer increased film adhesion through oxygen-to-oxygen bonding. Overall, for better properties, the optimal oxygen partial pressure and annealing temperature were 10% and 900 °C, respectively. Further improvement can be achieved by protective layers, such as glazes, aluminum oxide, and so on to reduce agglomeration and film loss at high temperature.

**Author Contributions:** Conceptualization, Y.P. and C.Z.; methodology, Y.P.; validation, Y.P., N.Z., L.S. and Y.R.; formal analysis, N.Z. and Y.R.; investigation, Y.P.; resources, Y.R. and C.Z.; data curation, Y.R. and N.Z.; writing—original draft preparation, Y.P.; writing—review and editing, N.Z.; visualization, L.S. and Y.R.; supervision, Y.R.; project administration, C.Z.; funding acquisition, C.Z. All authors have read and agreed to the published version of the manuscript.

**Funding:** This research was funded by the National Key Research and Development Program of China [2020YFB2009102].

**Institutional Review Board Statement:** Not applicable.

**Informed Consent Statement:** Not applicable.

**Data Availability Statement:** Not applicable.

**Acknowledgments:** The authors thank the Shanghai Electric Institute and School of Naval Architecture, Ocean & Civil Engineering for film adhesion testing experiments, the Center for Advanced Electronic Material and Devices for SEM and XRD measurement, and Limin Sun in the Instrumental Analysis Center of Shanghai Jiao Tong University for TOF-SIMS characterization.

**Conflicts of Interest:** The authors declare no conflict of interest.

## References

1. Li, M.; Hu, T. Research status and development trend of MEMS S&A devices: A review. *Def. Technol.* **2020**, *17*, 450–456.
2. Lin, X.; Zhang, C.; Yang, S.; Guo, W.; Zhang, Y.; Yang, Z.; Ding, G. The impact of thermal annealing on the temperature dependent resistance behavior of Pt thin films sputtered on Si and Al<sub>2</sub>O<sub>3</sub> substrates. *Thin Solid Film.* **2019**, *685*, 372–378. [[CrossRef](#)]
3. Zhao, X.; Yan, S.; Wang, H.; Jiang, H.; Zhang, W. Fabrication and microstructure evolution of Al<sub>2</sub>O<sub>3</sub>/ZrBN-SiCN/Al<sub>2</sub>O<sub>3</sub> high-temperature oxidation-resistant composite coating. *Ceram. Int.* **2019**, *45*, 247–251. [[CrossRef](#)]
4. Tsutsumi, K.; Yamashita, A.; Ohji, H. The experimental study of high TCR Pt thin films for thermal sensors. In Proceedings of the Sensors, 2002 IEEE, Orlando, FL, USA, 12–14 June 2002; pp. 1002–1005.
5. Purkl, F.; English, T.; Yama, G.; Provine, J.; Kenny, T.W. Sub-10 nanometer uncooled platinum bolometers via plasma enhanced atomic layer deposition. In Proceedings of the IEEE International Conference on Micro Electro Mechanical Systems, Taipei, Taiwan, 20–24 January 2013.
6. Rusanov, R.; Rank, H.; Fuchs, T.; Mueller-Fiedler, R.; Kraft, O. Reliability characterization of a soot particle sensor in terms of stress- and electromigration in thin-film platinum. *Microsyst. Technol.* **2016**, *22*, 481–493. (In English) [[CrossRef](#)]
7. Fricke, S.; Friedberger, A.; Seidel, H.; Schmid, U. A robust pressure sensor for harsh environmental applications. *Sens. Actuators A Phys.* **2012**, *184*, 16–21. [[CrossRef](#)]
8. Mattox, D.M. Influence of Oxygen on the Adherence of Gold Films to Oxide Substrates. *J. Appl. Phys.* **1966**, *37*, 3613–3615. [[CrossRef](#)]
9. Schmidl, G.; Dellith, J.; Kessler, E.; Schinkel, U. The influence of deposition parameters on Ti/Pt film growth by confocal sputtering and the temperature dependent resistance behavior using SiO<sub>x</sub> and Al<sub>2</sub>O<sub>3</sub> substrates. *Appl. Surf. Sci.* **2014**, *313*, 267–275. [[CrossRef](#)]
10. Sreenivas, K.; Reaney, I.; Maeder, T.; Setter, N.; Jagadish, C.; Elliman, R.G. Investigation of Pt/Ti bilayer metallization on silicon for ferroelectric thin film integration. *J. Appl. Phys.* **1994**, *75*, 232–239. [[CrossRef](#)]
11. Weng, S.; Qiao, L.; Wang, P. Thermal stability of Pt-Ti bilayer films annealing in vacuum and ambient atmosphere. *Appl. Surf. Sci. A J. Devoted Prop. Interfaces Relat. Synth. Behav. Mater.* **2018**, *444*, 721–728. [[CrossRef](#)]
12. Martin, D.M.; Agham, P.; Thong, Q.N.; Ajit, D.; David, J.S.; Alexander, A.D.; John, G.E. Growth of epitaxial oxides on silicon using atomic layer deposition: Crystallization and annealing of TiO<sub>2</sub> on SrTiO<sub>3</sub>-buffered Si(001). *J. Vac. Sci. Technol. B. Nanotechnol. Microelectron. Mater. Process. Meas. Phenom. JVST B* **2012**, *30*, 04E111-1–04E111-6. (In English)
13. Halder, S.; Schneller, T.; Waser, R. Enhanced stability of platinized silicon substrates using an unconventional adhesion layer deposited by CSD for high temperature dielectric thin film deposition. *Appl. Phys. A. Mater. Sci. Process.* **2007**, *87*, 705–708. (In English) [[CrossRef](#)]

14. Ababneh, A.; Al-Omari, A.N.; Dagamseh, A.M.K.; Tantawi, M.; Pauly, C.; Mücklich, F.; Feili, D.; Seidel, H. Electrical and morphological characterization of platinum thin-films with various adhesion layers for high temperature applications. *Microsyst. Technol.* **2015**, *23*, 703–709. [[CrossRef](#)]
15. Schmid, U.; Seidel, H. Effect of high temperature annealing on the electrical performance of titanium/platinum thin films. *Thin Solid Films* **2008**, *516*, 898–906. [[CrossRef](#)]
16. Courbat, J.; Briand, D.; Rooij, N. Reliability improvement of suspended platinum-based micro-heating elements. *Sens. Actuators A Phys.* **2008**, *142*, 284–291. [[CrossRef](#)]
17. Garraud, A.; Combette, P.; Giani, A. Thermal stability of Pt/Cr and Pt/Cr<sub>2</sub>O<sub>3</sub> thin-film layers on a SiN<sub>x</sub>/Si substrate for thermal sensor applications. *Thin Solid Films* **2013**, *540*, 256–260. [[CrossRef](#)]
18. Chung, G.S.; Kim, C.H. RTD characteristics for micro-thermal sensors. *Microelectron. J.* **2008**, *39*, 1560–1563. [[CrossRef](#)]
19. Kuribayashi, K.; Kitamura, S. Preparation of Pt-PtO<sub>x</sub> thin films as electrode for memory capacitors. *Thin Solid Films* **2001**, *400*, 160–164. [[CrossRef](#)]
20. Budhani, R.C.; Prakash, S.; Bunshah, R.F. Thin-film temperature sensors for gas turbine engines: Problems and prospects. *J. Vac. Sci. Technol. A Vac. Surf. Film.* **1986**, *4*, 2609–2617. [[CrossRef](#)]
21. John, D.W.; Kimala, L.H. *Preparation and Analysis of Platinum Thin Films for High Temperature Sensor Applications*; National Aeronautic Space Administration (NASA): Washington, DC, USA, 2005.
22. Grosser, M.; Schmid, U. The impact of annealing temperature and time on the electrical performance of Ti/Pt thin films. *Appl. Surf. Sci.* **2010**, *256*, 4564–4569. [[CrossRef](#)]
23. Schssler, T.; Schn, F.; Lemier, C.; Urban, G. Effect of high temperature annealing on resistivity and temperature coefficient of resistance of sputtered platinum thin films of SiO<sub>2</sub>/Pt/SiO<sub>x</sub> interfaces. *Thin Solid Films* **2020**, *698*, 137877. [[CrossRef](#)]
24. Pang, Y.; Zhang, C.; Lei, P.; Wang, Y.; Lv, Z. Effects of Thermal Annealing on the Electrical Properties and Stability of Pt Thin Film Resistors with Ti and Pt<sub>x</sub>O<sub>y</sub> Interlayers. *J. Phys. Conf. Ser.* **2021**, *2002*, 012002. [[CrossRef](#)]
25. Firebaugh, S.L.; Jensen, K.F.; Schmidt, M.A. Investigation of high-temperature degradation of platinum thin films with an in situ resistance measurement apparatus. *J. Microelectr. Syst.* **1998**, *7*, 128–135. [[CrossRef](#)]
26. Jiran, E.; Carl, V. Thompson. Capillary instabilities in thin films. *J. Electron. Mater.* **1990**, *19*, 1153–1160. [[CrossRef](#)]
27. Berry, R.J. Effect of Pt Oxidation on Pt Resistance Thermometry. *Metrologia* **1980**, *16*, 117–126. [[CrossRef](#)]
28. Niu, Y.L.; Song, K.; Sun, J.P.; Xu, L.I.; Meng, Y.E. Research on the Decomposition Experiment of PtO<sub>2</sub> in Air Environment. *Acta Metrol. Sin.* **2018**, *39*, 33–38.
29. Mooiman, M.B.; Sole, K.C.; Dinham, N. The Precious Metals Industry: Global Challenges, Responses, and Prospects. In *Metal Sustainability: Global Challenges, Consequences, and Prospects*; John Wiley & Sons, Ltd.: Hoboken, NJ, USA, 2016.
30. Joseph, R.D. Precious Metals and Alloys. In *Metals Handbook Desk Edition*; ASM International: Almere, The Netherlands, 1998. [[CrossRef](#)]
31. Kumar, M.; Kumar, T.; Pandey, R.K.; Pathak, S.; Kumar, R. Roughening and Sputtering Kinetics of Pt Thin Films at different Angles of Ion Irradiation. *Mater. Lett.* **2021**, *303*, 130474. [[CrossRef](#)]
32. Ruina, J.; Kunlun, W.; Yanqing, X.; Hui, S.; Jianhong, G.; Lan, Y.; Yong, W. Enhancing the temperature coefficient of resistance of Pt thin film resistance-temperature-detector by short-time annealing. *Ceram. Int.* **2023**, *49*, 12596–12603.
33. Zhang, Y.; Ba, D.; Liu, X.; Hang, G. Latest Progress in Development of Thin Film Temperature Sensors. *Vac. Sci. Technol.* **2003**, *23*, 334–1124.

**Disclaimer/Publisher’s Note:** The statements, opinions and data contained in all publications are solely those of the individual author(s) and contributor(s) and not of MDPI and/or the editor(s). MDPI and/or the editor(s) disclaim responsibility for any injury to people or property resulting from any ideas, methods, instructions or products referred to in the content.